OH Formation in the Photoexcitation of NO_2 beyond the Dissociation Threshold in the Presence of Water Vapor

John N. Crowley* and Shaun A. Carl

Max-Planck Institut für Chemie, Division of Atmospheric Chemistry, Postfach 3060, 55020 Mainz, Germany

Received: January 24, 1997; In Final Form: April 3, 1997[⊗]

The pulsed-laser-excitation/resonance fluorescence technique was used to assess the efficiency of OH formation following photoexcitation of NO_2 at discrete wavelengths beyond the photodissociation threshold in the presence of water vapor: $NO_2^* + H_2O \rightarrow HONO + OH$. Excitation at wavelengths between 432 and 449 nm was found to lead to OH production via a facile sequential two-photon absorption by NO_2, leading to $O(^1D)$ and thus to OH in the presence of H_2O, i.e., $NO_2 + h\nu \rightarrow NO_2^*$, $NO_2^* + h\nu \rightarrow NO_2^{**}$, $NO_2^{**} \rightarrow NO + O(^1D)$, $O(^1D) + H_2O \rightarrow 2OH$. The cross section for the transition $NO_2^{**} \leftarrow NO_2^*$ was found to be similar to that for the $NO_2^* \leftarrow NO_2$ transition at 435 nm. At 532 nm, the two-photon process is not sufficiently energetic to form $O(^1D)$, and OH is not observed. An upper limit of approximately 7×10^{-5} is found for the reactive quenching of NO_2^* by water vapor relative to collisional quenching. The atmospheric relevance of OH formation via NO_2 excitation is discussed.

Introduction

The OH radical is the primary oxidant in the daytime troposphere, and its concentration determines the lifetimes and thus the abundance of most natural and anthropogenically emitted chemical species,[1] including hydrocarbons, CO, NO_2, and SO_2.

The photolysis of O_3 in the presence of water vapor is the major source of the OH radical.

$$O_3 + h\nu \rightarrow O_2 + O(^1D) \quad (1)$$

$$O(^1D) + H_2O \rightarrow 2OH \quad (2)$$

$$O(^1D) + M \rightarrow O(^3P) + M \quad (3)$$

The production rate of OH via O_3 photolysis is given by

$$R_{OH} = 2J(O_3)[O_3]/(1 + k_3[M]/k_2[H_2O]) \quad (i)$$

where $J(O_3)$ is the photolysis rate constant for O_3 and is equal to about 1×10^{-6} s^{-1} at high latitudes in winter, k_3 is the rate constant for collisional deactivation of $O(^1D)$ by air, and k_2 is the rate constant for reaction of $O(^1D)$ with H_2O. This expression yields OH production rates of 2×10^5 OH cm^{-3} s^{-1} if $[O_3] = 0.05$ ppm, and an H_2O pressure of 10 Torr is assumed.

Tropospheric O_3 concentrations are influenced by fast gas-phase photochemical cycles[2] involving NO_2. NO_2 absorbs sunlight strongly and is in rapid photochemical equilibrium (photostationary state) with NO_x and O_3 ($NO_x = NO + NO_2$).

$$NO_2 + h\nu \rightarrow NO + O \quad (4)$$

$$O + O_2 + M \rightarrow O_3 + M \quad (5)$$

$$NO + O_3 \rightarrow NO_2 + O_2 \quad (6)$$

The steady-state O_3 concentration is given by

$$[O_3] = J(NO_2)[NO_2]/k_6[NO] \quad (ii)$$

where $J(NO_2)$ is the rate constant for photolysis to $O(^3P) + NO$ (4).

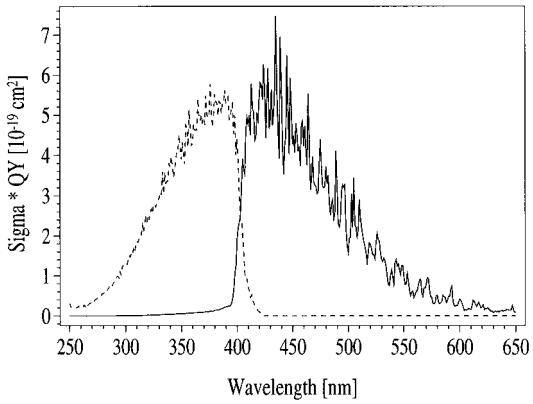

Figure 1. The UV/vis absorption spectrum (Sigma) of NO_2 multiplied by the quantum yield (QY) for dissociation to $O(^3P) + NO(^2\Pi)$ (dotted line) and by the quantum yield for photoexcitation to NO_2^* (solid line).

Additional reactions that oxidize NO to NO_2, e.g., with peroxy radicals,

$$NO + RO_2 \rightarrow NO_2 + RO \quad (7)$$

result in a net production of O_3 from NO_2 photolysis. The above discussion thus shows how OH, O_3, and NO_2 are closely linked in fast photochemical cycles.

The conditions under which O_3 loss or production terms dominate have been investigated in model calculations of the global troposphere,[3] and the critical concentration of NO at which O_3 formation is favored is estimated as about 10−20 ppt ($[NO_x] = 40$ ppt). Such low concentrations of NO_x are usually only found in very clean air. Recent estimates[4] suggest that about 65% of global tropospheric ozone is formed by the oxidation of NO by HO_2 and the subsequent photolysis of NO_2.

The absorption spectrum of NO_2 displays two broad continua centered at ca. 400 and 210 nm with underlying fine structure. In the troposphere the filtering effect of O_3 means that only light of wavelengths longer than about 300 nm is intense enough to initiate photochemistry. This paper therefore concentrates on excitation in the long wavelength continuum of NO_2 between about 400 and 600 nm.

The thermodynamic threshold for dissociation of NO_2 into $O(^3P)$ atoms and NO is 25 130 cm^{-1}, corresponding to a

[⊗] Abstract published in *Advance ACS Abstracts,* May 1, 1997.

S1089-5639(97)00319-8 CCC: $14.00

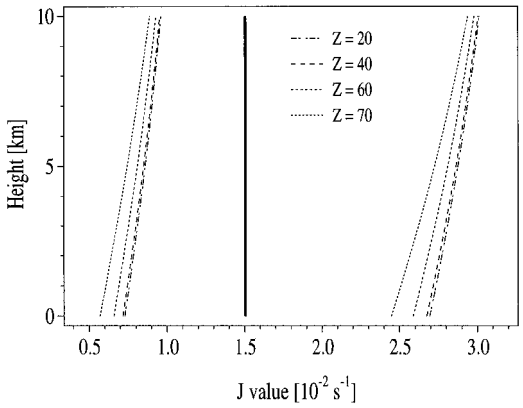

Figure 2. *J* values for photodissociation (left of solid vertical line) and for photoexcitation (right of solid vertical line). J values are given for zenith angles (*Z*) of between 20° and 70° and at altitudes of 0−10 km.

wavelength of 398 nm.[5] The experimental observations indicate that O atom production takes place out to 424 nm, where excess energy is provided by a combination of rovibrational excitation and energy transfer from bath-gas molecules.[6] The complexity of the NO_2 spectrum is due to strong coupling between the $^2A_1$ ground state and the $^2B_1$ and $^2B_2$ excited states, yielding optically excited states that have considerable ground electronic state character. The high density of states results in an excited-state radiative lifetime (τ_{rad}) of between 30 and 200 μs,[7−9] depending upon excitation wavelength. In contrast, the lifetime of the dissociative state[10] is close to 1×10^{-13} s. Figure 1 shows the absorption spectrum of NO_2 between 250 and 650 nm, multiplied by the wavelength-dependent quantum yields.[6] The dotted line thus represents dissociation to NO and $O(^3P)$ and the solid line excitation to longer lived excited states which we designate as NO_2*.

$$NO_2 + h\nu \rightarrow NO_2^* \tag{8}$$

Although the integrated areas of the dissociative and nondissociative parts of the spectrum are similar, the solar spectrum shows a strong wavelength dependence in this region with a large increase in ground level irradiance going from 320 to 450 nm when the solar zenith angles are large (e.g., in the winter troposphere). The relative rates of photodissociation (and thus $O(^3P)$ production) to photoexcitation were calculated by convoluting the dotted and solid parts of the NO_2 spectrum of Figure 1 with the solar spectrum.[11] For a zenith angle of >70°, the photoexcitation of NO_2 is calculated to proceed at a rate about 5 times that of photodissociation. The results are summarized in Figure 2. The fate of the excited NO_2* will be determined by its fluorescence lifetime (τ_{rad}) or quenching by the major bath gases N_2, O_2, or H_2O. The quenching rate constants have been measured as 2.7×10^{-11}, 3.0×10^{-11}, and 1.7×10^{-10} cm^3 molecule^{-1} s^{-1} for N_2, O_2, and H_2O, respectively.[5] At ground level the total quenching rate is 7.1×10^8 s^{-1}, resulting in a NO_2* lifetime of about 1.4 ns which is thus controlled almost exclusively by collisional quenching.

$$NO_2^* + M \rightarrow NO_2 \tag{9}$$

As the quenching rate constants show, H_2O is a particularly efficient quencher of NO_2* and, despite its lower concentration when compared to N_2 and O_2 in the troposphere, contributes about 8% to the total quenching rate if we assume 150 Torr of O_2, 600 Torr of N_2, and 10 Torr of H_2O. A NO_2* molecule that has absorbed a photon of wavelength 440 nm has 65 kcal/mol energy over that of ground-state NO_2. If all of this energy can be carried into the reaction with H_2O (i.e., no internal relaxation before collision), we find that the generation of OH radicals and HONO becomes a thermodynamically feasible reactive quenching mechanism ($\Delta H_r(10) = -25$ kcal/mol)

$$NO_2^* + H_2O \rightarrow OH + HONO \tag{10}$$

Note that $\Delta H_r(10)$ is calculated for products formed in the electronic ground state, $OH(^2\Pi)$ and $HONO(^1A)$, whereby spin is conserved. Even at wavelengths greater than 600 nm, the photon energy is sufficient to make reaction 10 exothermic. By contrast, the reaction of ground-state NO_2 with H_2O to yield HONO and OH is 40 kcal/mol endothermic.

Some evidence already exists for the enhanced reactivity of electronically excited NO_2, which reacts with ground-state NO_2 to give either $2NO + O_2$[12−14] or $NO_3 + NO$.[15,16]

$$NO_2^* + NO_2 \rightarrow 2NO + O_2 \tag{11a}$$

$$\rightarrow NO_3 + NO \tag{11b}$$

Both of these reactions are endothermic for interaction between two ground-state NO_2 species. In addition, small yields of N_2O have been observed[17] in the reactive collisional quenching of NO_2* by N_2. Thus, should NO_2* also react with H_2O, a mechanism for the NO_2-initiated generation of OH radicals in the troposphere is available that bypasses the formation of O_3 and its photolysis to $O(^1D)$, which in the winter months at low zenith angles is slow due to the reduced solar flux at the shorter wavelengths.

Under these circumstances, the rate of OH production is given by

$$R_{OH} = J_{ex}(NO_2)[NO_2]/(1 + k_9[M]/k_{10}[H_2O]) \tag{iii}$$

where $J_{ex}(NO_2)$ is the rate constant for nondissociative excitation of NO_2, k_9 is the quenching rate constant of NO_2* by air, and k_{10} is the rate constant for reaction of NO_2* with H_2O.

Assuming a NO_2 concentration of 1 ppb and an O_3 concentration of 0.05 ppm, an excitation rate that is 5 times the photolysis rate, $J_{ex}(NO_2) = 2 \times 10^{-2}$ s^{-1}, and that HONO is also rapidly photolyzed to OH and NO, then the rate constant for NO_2* + H_2O (k_{10} in the above text) which is necessary to generate OH at the same rate as O_3 photolysis is found to be 4×10^{-13} cm^3 molecule^{-1} s^{-1}. This rate constant is about 0.2% of the quenching rate constant for NO_2* with H_2O. Thus, if only 2 per mil of excited NO_2 is reactively quenched by H_2O (10) rather than collisionally quenched (12), the reaction between NO_2* and H_2O would represent an equally important source of OH in the (weakly illuminated) winter troposphere as the photolysis of O_3 and the subsequent reaction of $O(^1D)$ with H_2O.

$$NO_2^* + H_2O \rightarrow NO_2 + H_2O \tag{12}$$

In addition, the rate of NO_2* formation via NO + O_3 will increase the rate of NO_2* formation by about 10% under the conditions of NO_2 and O_3 given above and assuming about 50 ppt NO.

Photochemical experiments in environmental smog chambers have been carried out for many years with the goal of deriving reaction mechanisms for tropospheric oxidation processes and to validate computer models of air pollution. As in the atmosphere, OH radicals are often the primary oxidant. Several publications have drawn attention to unknown radical sources in smog chamber experiments, which have been attributed to the formation (and subsequent photolysis) of HONO via a surface reaction of NO_2 and H_2O[18] or between HNO_3 and NO.[19]

Experiments have also shown that not only the rate of OH formation but that of HONO formation is dependent on the intensity of irradiation by UV−vis light.[20] The explanation given requires a photoenhancement in the rate of the heterogeneous $NO_2 + H_2O$ reaction taking place on the walls of the reactor. We note that reaction 10 would provide an alternative mechanism for HONO and OH formation as observed in those experiments.

To investigate the possibility that reactive quenching of NO_2* by H_2O to form OH and HONO can play a role in the troposphere (and in smog chamber experiments), we have carried out experiments to investigate the formation of OH in the pulsed-laser photoexcitation of NO_2 in the presence of H_2O vapor.

Experimental Section

Formation of OH in the reaction between NO_2* and H_2O was investigated by the method of pulsed-laser-excitation/resonance fluorescence. Pulsed, tunable radiation of wavelengths between 430 and 450 nm (line width = 0.15 cm^{-1}) was obtained by pumping a Lambda Physik Scanmate-2 dye laser with either a Nd:YAG laser (Quantel Brilliant B, pulse width = 5 ns) or with an excimer laser (Lambda Physik Lextra 50, pulse width = 20 ns). The dye used, coumarin 120, was excited at 355 nm (Nd:YAG pump) or 351 nm (XeF excimer pump) at repetition rates of between 5 and 10 Hz. The dye laser beam was expanded to 5 mm diameter and reduced to ca. 4 mm diameter by a set of irises before entering the Teflon-coated stainless steel reaction vessel[21] through quartz windows at the Brewster angle. The intensity was monitored with a calibrated joule meter upon exiting through a second Brewster window.

The pulse energy of the pump laser was varied to provide photon fluences of typically between 3 and 14 mJ/cm^2 for expanded laser beams of 4 mm diameter. Some experiments were also carried out at 532 nm by coupling the second harmonic of the Nd:YAG laser directly into the reaction vessel through the same set of irises. For those experiments in which the Nd:YAG laser was used to pump the dye laser, the excimer laser was run with ArF to generate 193 nm pulses. The 193 nm radiation was coupled into the reaction vessel via a beam splitter, through the same irises, and was used to dissociate N_2O in the presence of H_2O vapor to provide a calibration signal for OH (see below).

NO_2 was diluted as a ca. 5% mixture in Ar and its flow regulated by a mass flow controller. A second, calibrated, Ar flow was directed through a H_2O-filled bubbler at room temperature and through a glass spiral maintained at temperatures between 1 and 5 K below that of the bubbler to ensure saturation. The resultant H_2O/Ar mixture was mixed with the NO_2/Ar flow and a third calibrated flow of pure Ar before being directed into a long-path optical absorption cell connected in series to the RF cell. Absorption of light from a halogen lamp over a path length of 975 cm was detected by a diode-array detector and was used to determine the NO_2 concentration. In some experiments, the attenuation of the laser light upon addition of the NO_2 flow to the reaction volume was measured using the joule meter. In combination with the literature value of the absorption cross section of NO_2 at the excitation wavelength and the optical path between the two Brewster windows (≈18 cm), this enabled the NO_2 concentration to be determined. The values obtained were consistent with the [NO_2] measurement described above, but was useful only for high [NO_2] when the averaged joule meter reading was sufficiently accurate to detect the small absorption over 18 cm. The amount of NO_2 that was promoted into the excited state following the laser pulse was calculated from the concentration of NO_2, the measured photon fluence, and the known absorption cross section at the excitation wavelength.

OH generated in the laser pulse were excited using an OH resonance lamp to promote the $OH(^2\Sigma^+) \leftarrow OH(^2\Pi)$ transition at ≈309 nm. The mildly focused light from the resonance lamp crossed the laser beam at the focal point of a telescopic lens system which directed resonantly scattered photons to a photon-counting photomultiplier. The calibration of OH was achieved by replacing the $NO_2/H_2O/Ar$ flow with one of $N_2O/H_2O/Ar$ at the same flow rate and total pressure of H_2O and Ar to preserve the resonance fluorescence sensitivity, which is dependent on the quenching of $OH(^2\Sigma^+)$. The $N_2O/Ar/H_2O$ mixture, containing about 3×10^{15} molecules cm^{-3} of N_2O, was photolyzed at 193 nm using an identical beam geometry as in the 430−450 and 532 nm experiments. Using the well-known N_2O cross section at 193 nm, and a quantum yield for OH formation of 2, the concentration of OH could be determined via the calculated extent of N_2O dissociation. This required knowledge of the laser fluence at 193 nm, which was measured using the joule meter. A small correction (<5%) was applied to take into account the loss of OH via reaction of $O(^1D)$ with N_2O (k_2/k_{13} = 1.9 [22]) and also the photolysis of H_2O.

$$N_2O + h\nu\ (193\ nm) \rightarrow N_2 + O(^1D) \quad (13)$$

$$O(^1D) + H_2O \rightarrow 2OH \quad (2)$$

$$O(^1D) + N_2O \rightarrow \text{products} \quad (14)$$

The conditions most conducive to optimize the amount of NO_2* that is quenched by H_2O rather than bath gas were those of maximum H_2O vapor pressure. However, the sensitivity of the resonance fluorescence detection of OH decreased rapidly with increasing H_2O partial pressure due to the very high quenching rate constant[23] for $OH(^2\Sigma^+)$ with H_2O of $(2-5) \times 10^{-10}$ cm^3 $molecule^{-1}$ s^{-1}. Similarly, N_2 is a much more efficient quencher of $OH(^2\Sigma^+)$ than Ar and at a pressure of 20 Torr was found to reduce the OH signal to just 20% of that obtained in the same pressure of Ar. These considerations therefore constrained the experimental conditions to total pressures of Ar bath gas of about 20 Torr and H_2O concentrations of 2 Torr or below. The quenching rate constants for NO_2* by H_2O and Ar are 1.7×10^{-10} and 1.85×10^{-11} cm^3 $molecule^{-1}$ s^{-1}, respectively.[5] The first-order loss rates for NO_2* is thus 2×10^4 s^{-1} for fluorescence (based on τ_{rad} = 50 μs), 1.1×10^7 s^{-1} for quenching by 19 Torr of Ar, and 5.8×10^6 s^{-1} for quenching by 1 Torr of H_2O. This means that 33% of the NO_2* is quenched by H_2O under the experimental conditions. (Self-quenching by NO_2 could be neglected as its concentration is too low.) The quenching rate constants of NO_2* by Ar and He are almost identical, and quenching of $OH(^2\Sigma^+)$ by both gases is very small.[23] Ar was therefore used in preference of He to reduce diffusion. The typical total flow rate was about 250 sccm (cm^3 (STP) min^{-1}), resulting in a total pressure in the UV cell of 24 Torr and in the fluorescence cell of 20 Torr. The residence time in the fluorescence cell was about 1 s (linear velocity = 8 cm s^{-1}) and 20 s in the UV cell.

NO_2, purchased as N_2O_4 (Merck, 99.5%), N_2O (Hoechst, 99.5%), H_2O (distilled, Millipore), CH_4 (Linde 99.9%), and Ar (Linde 99.999%) were used without further purification.

Results

432−449 nm Excitation. Figure 3 displays fluorescence intensity as a function of time following the pulsed photolysis

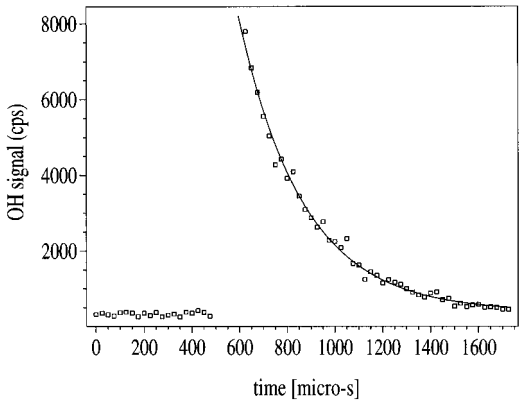

Figure 3. Production and decay of OH following 439.4 nm photolysis of a flowing $NO_2/H_2O/Ar$ mixture. The solid line is a pseudo-first-order fit to the decay as described in the text. The integration time per channel was 25 μs; 3000 laser pulses were averaged at 10 Hz. cps = counts per second.

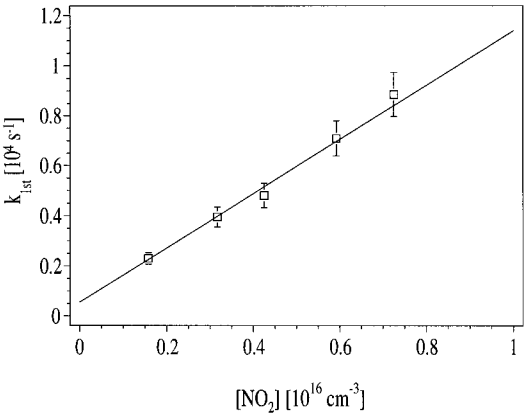

Figure 4. Dependence of the pseudo-first-order decay rate (k_{1st}) of OH on the initial concentration of NO_2. The fit to the data gives a rate constant for OH + NO_2 of $(1.1 \pm 0.1) \times 10^{-12}$ cm^3 molecule^{-1} s^{-1} at 20 Torr of Ar and at 295 K. The error bars are statistical (2σ).

(5 ns pulse) of a flowing mixture of $NO_2/Ar/H_2O$ at 439.4 nm. The total pressure was 20 Torr with 19 Torr of Ar, 1 Torr of H_2O, and $[NO_2] = 3.33 \times 10^{15}$ molecules cm^{-3}. The measured fluence was 14 mJ cm^{-2}. The laser was triggered at time = 500 μs in this trace. Twenty channels of data (500 μs) were acquired prior to the pulse to establish the intensity of background scattered light from the resonance lamp. Once corrected for this background signal, the decays were found to be exponential and the decay rate linearly dependent on the initial NO_2 concentration. Stray light following the laser pulse precluded the analysis of the data up to 75 μs after the 20 ns pulse was complete, and these data were not included in the nonlinear least-squares fit to the data represented by the solid line in Figure 3.

The background-corrected data were fit to an algorithm of the form

$$[OH]_t = [OH]_0 \exp(-k_{1st}t) \qquad \text{(iv)}$$

where k_{1st} is the pseudo-first-order decay constant (in s^{-1}) of OH and is defined as $k_{1st} = k_{bi}[NO_2]$, where k_{bi} is the bimolecular rate constant for the reaction of OH with NO_2 at the given temperature and pressure.

A plot of pseudo-first-order decay rate versus the optically determined $[NO_2]_0$ (Figure 4) yields a rate constant of $k_{bi} = (1.1 \pm 0.1) \times 10^{-12}$ cm^3 molecule^{-1} s^{-1}. This is close to the literature rate constant for the reaction between OH and NO_2

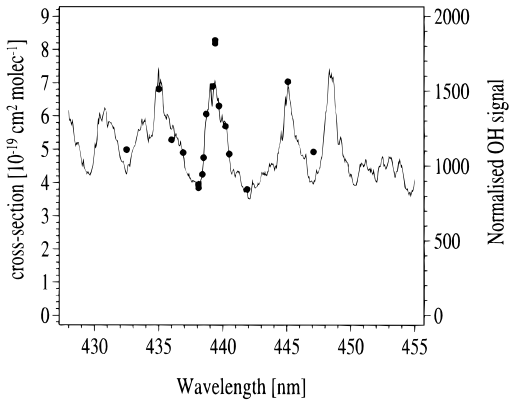

Figure 5. The 420−460 nm visible absorption spectrum of NO_2 (line, left *y*-axis) and the OH signal height as a function of excitation wavelength (solid circles, right *y*-axis). The OH signal has been normalized for the number of photons per pulse, signal integration time, and laser fluence squared.

at the experimental temperature and pressure in air (1.3×10^{-12} cm^3 molecule^{-1} s^{-1}) and confirms that the detected species is OH.

Having established that OH is formed in the 439.4 nm photolysis of $NO_2/Ar/H_2O$ mixtures, a series of diagnostic tests were carried out to ascertain whether reaction 10 is its source. Figure 5 shows a plot of initial OH signal intensity as a function of wavelength for a small section of the NO_2 spectrum. The OH signal is gained by back-extrapolation of the exponential decay of OH to $t = 0$ and has been normalized for number of laser pulses and integration time and the laser fluence squared (see below). The NO_2 concentration was held constant at about 2.5×10^{15} molecules cm^{-3} for the whole experiment; that of H_2O was held at ≈0.5 Torr. The measured laser fluence at each wavelength was converted to a number of photons/pulse to make comparison between each wavelength meaningful. There is clearly good correlation between the OH signal intensity and the features of the NO_2 spectrum, with maxima and minima in the OH signal correlating with peaks and troughs of the NO_2 spectrum, and confirms that the initial absorption process responsible for OH formation is by NO_2. Note however that this good agreement was only obtained when the OH signal was normalized to the squared laser energy; otherwise, the features of the NO_2 spectrum were reproduced, but the relative magnitude of the signal did not match.

The energy dependence of the OH signal was therefore measured as a function of laser fluence at a fixed wavelength (439.4 nm) and fixed NO_2 and H_2O concentrations similar to above. The results are displayed in Figure 6 in which the ln-(relative pulse energy) is plotted against the extrapolated ln-(signal) at $t = 0$ for experiments with the Nd:YAG laser used to pump the dye laser. The slope of the plot is 2.06 ± 0.12. For comparison, the slope for the same plot for 193 nm photolysis of a $N_2O/H_2O/Ar$ mixture yields a slope of 1.14 ± 0.15. A slope of unity is expected for a single-photon process, whereas a slope of two is expected for a two-photon process. Using the Nd:YAG or the excimer laser to pump the dye laser yielded identical slopes. An approximate dependence on the square of the initial NO_2* concentration could indicate not only two-photon absorption but also collisional interaction of two singly excited NO_2*. This could be ruled out by conducting experiments at fixed energy and varying the NO_2 concentration. In this case the dependence on $[NO_2]$ was found to be linear as shown in Figure 7.

The question remains how two-photon absorption by NO_2 can lead to OH formation in the $Ar/NO_2/H_2O$ mixture. Note

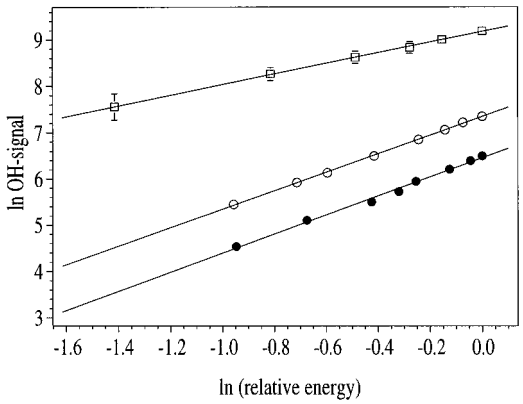

Figure 6. Dependence of $[OH]_0$ on the laser pulse energy. Open squares: 193 nm photolysis of N_2O /H_2O, slope = 1.14 ± 0.15. Full circles: 439.4 nm excitation of $NO_2/H_2O/Ar$, slope = 2.06 ± 0.12. Open circles: 439.4 nm excitation of $NO_2/H_2/Ar$, slope = 2.00 ± 0.04. The error bars are statistical (2σ) errors on the back-extrapolated OH signal at $t = 0$.

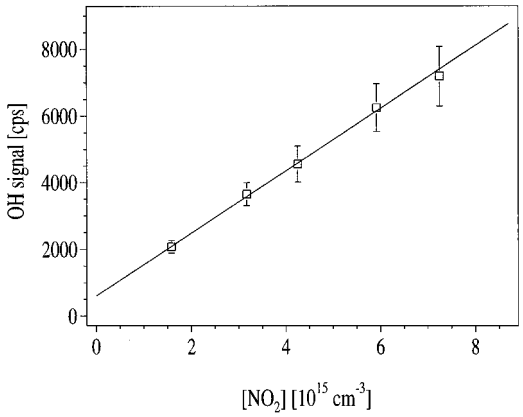

Figure 7. Dependence of $[OH]_0$ generated by photolysis at 435 nm on the initial NO_2 concentration. The OH signal is normalized for total integration time (cps = counts per second). Error bars are statistical error (2σ) on the back-extrapolated OH signal.

that the action spectrum for OH formation matches the structure in the NO_2 absorption spectrum, implying that sequential two-photon absorption is taking place. Simultaneous two-photon absorption is in any case highly unlikely considering the low photon densities in the unfocused laser beam (e.g., at 10 mJ/cm^2 and 20 ns pulse, the irradiance is 5×10^9 J s^{-1}m^{-2} and the photon density is calculated as 4×10^{13} photons cm^{-3}). We suggest that a transition from the initially populated, mixed NO_2*($^2B_1/^2B_2/^2A_1$) state to the dissociative NO_2**($2\ ^2B_2$) state is possible at wavelengths close to 440 nm. This is an allowed transition due to the partial ground-state nature of the NO_2* excited state and corresponds to absorption of a single photon of wavelength close to 220 nm to the $2\ ^2B_2$ state, as has been observed in absorption spectroscopic studies. The $2\ ^2B_2$ state dissociates to give $O(^1D)$ and $NO(^2\Pi)$ with a single-photon absorption threshold of 244 nm,[5] although yields of $O(^3P)$ remain substantial at wavelengths between 214 and 239 nm with the $O(^1D)$ yield close to 40%.[24]

$O(^1D)$ is thus identified as the source of OH via reaction 2. As a test of this supposition, experiments were carried out in which H_2O was replaced by CH_4. The rate constants for reaction of $O(^1D)$ with H_2O and CH_4 are 2.2×10^{-10} and 1.7×10^{-10} cm^3 molecule^{-1} s^{-1}, respectively, and H_2O and CH_4 pressures of 0.5 and 0.65 Torr were chosen to ensure that the relative rates of quenching of $O(^1D)$ with Ar (the quenching rate constant with Ar is 7.0×10^{-13} cm^3 molecule^{-1} s^{-1}) and reaction with H_2O or CH_4 were kept constant. The results of

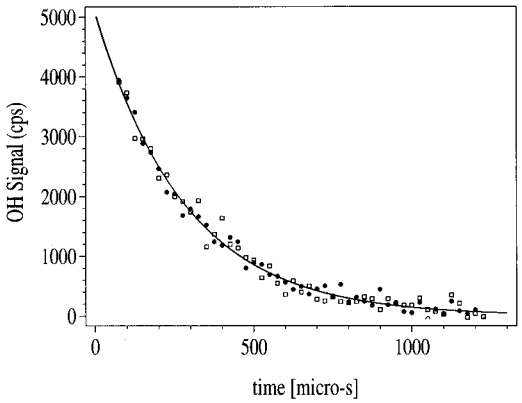

Figure 8. OH generated in the 435 nm photolysis of $NO_2/H_2O/Ar$ (solid circles) or $NO_2/CH_4/Ar$ (open squares). Concentrations are given in the text. cps = counts per second.

an experiment in which ca. 4×10^{15} molecules cm^{-3} of NO_2 was photolyzed at 435 nm in the presence of either 0.5 Torr of H_2O and 20 Torr of Ar or 0.65 Torr of CH_4 and 20 Torr of Ar are displayed in Figure 8. The OH profiles in both experiments are clearly very similar, and as there is no obvious route to OH formation via a reaction of NO_2* in the CH_4 experiments, we conclude that $O(^1D)$ is responsible in both cases. The almost identical magnitude of the initial OH signal in both experiments is thought to be fortuitous and is probably the result of the greater quantum yield of OH production in the reaction of $O(^1D)$ with H_2O being compensated by the lower quenching rates of NO_2* and possibly also reduced quenching of $OH(^2\Sigma^+)$ by CH_4 as compared to H_2O. Experiments were also carried out in which H_2O was replaced by H_2. Again OH was observed, and the dependence upon energy was determined. The plot of relative energy versus OH signal yielded a slope of 2.00 ± 0.04, and we conclude that the two-photon formation of $O(^1D)$ and reaction with H_2 are responsible. These data are also shown in Figure 6. In this case a stronger OH signal is seen due to the formation of a second OH radical by

$$O(^1D) + H_2 \rightarrow OH + H \quad (15)$$

$$H + NO_2 \rightarrow OH + NO \quad (16)$$

Previous experiments have also identified two-photon effects in the beyond-threshold dissociation of NO_2,[25,26] and have shown that pulsed (10 ns) laser excitation of the $^2B_2$ state (693.4 nm) with laser energies between 1 and 2 J (giving rise to photon densities approximately 2 orders of magnitude greater than in the present study) results in $O(^3P)$ generation. As in the present study, sequential two-photon absorption was thought to be responsible.

Taking the data from a typical $NO_2/Ar/H_2O$ experiment in which the OH concentration was calibrated, we can derive the approximate cross section for the absorption of the second photon by NO_2*. With a starting concentration of $[NO_2] = 2.8 \times 10^{15}$ molecules cm^{-3} and a photon fluence of 13.6 mJ cm^{-2} at 439.4 nm and by using the known absorption cross section of NO_2 ($\sigma = 7.08 \times 10^{-19}$ cm^2 molecule^{-1}), we calculate that 6.0×10^{13} molecules cm^{-3} NO_2* is generated in the pulse. As the identical slopes were obtained for Nd:YAG or excimer pumps, quenching of NO_2* must be negligible within the duration of the laser pulse (5 or 20 ns, respectively). In addition, quenching of $O(^1D)$ by Ar is negligible compared to reaction with H_2O, and we assume that the concentration of OH (8.4×10^{11} molecules cm^{-3}) is the same as the number of photons absorbed by NO_2* per unit volume. (A small correction of <10% is necessary to take into account reaction of $O(^1D)$ with

NO_2 that does not give OH.) This of course also assumes that all NO_2** dissociates to $O(^1D)$. If, however, we equate NO_2** with the 2 $^2B_2$ state, and assume that the $O(^1D)$ yields obtained by direct excitation[24] at 214−239 nm are applicable here, then the OH generated represents only about 40% of the total NO_2* excited. We thus derive a very approximate cross section of ca. 5×10^{-19} cm^2 molecule^{-1} for absorption of a photon of wavelength 439.4 nm by NO_2*. Consistent results (±20%) were obtained when the laser fluence was halved to 6.8 mJ/cm^2 with [NO_2] held constant and when the NO_2 concentration was increased to 4.9×10^{15} molecules cm^{-3} with the laser fluence (16.6 mJ/cm^2) held constant. Large potential errors on this cross section arise from the indirect estimation of [NO_2*] and [OH] via joule meter measurements of laser fluence and assumptions concerning the yield of $O(^1D)$ from NO_2**. The magnitude of the cross section appears, however, to be similar that for absorption of a similar frequency photon by ground-state NO_2.

Sequential two-photon absorption and $O(^1D)$ formation also most probably occurred in the experiments of Nizkorodov et al.,[16] who used photon fluences at 436.45 nm that were up to a factor of 5 greater than in the present work. The linear dependence of NO_3 formation on pulse energy observed by these authors probably reflects the minor role of this process compared to the NO_2* + NO_2 reaction to give NO_3 in the photolysis of pure NO_2 samples,

532 nm Excitation. The interfering feature of the two-photon process is that it generates OH via $O(^1D)$. The thermodynamic threshold for two-photon generation of $O(^1D)$ from NO_2 excitation is 488 nm. This is calculated from the known 244 nm threshold for $O(^1D)$ production via one photon and assuming no internal relaxation of NO_2* before the second photon is absorbed. Thus, although excitation at $\lambda > 488$ nm may involve two-photon absorption, this cannot lead to $O(^1D)$, but possibly to $O(^3P)$ formation as previously observed.[25,26] Experiments were therefore carried out with excitation at 532 nm, by coupling the second harmonic of the Nd:YAG laser directly into the reaction cell. The cross section of NO_2 at 532 nm is smaller than that around 400−450 nm ($\sigma_{532} = 1.44 \times 10^{-19}$ cm^2 molecule^{-1}), but two-photon absorption no longer presents a limitation to the photon fluence, and the low cross section can be compensated by high pulse energies to ensure sufficient population of NO_2*.

A flowing mixture of [NO_2] = 4.4×10^{15} molecules cm^{-3} (measured by visible absorption), 2 Torr of H_2O, and 16 Torr of Ar was irradiated with 157 mJ/cm^2 per pulse at 532 nm. Under these conditions, about 2.7×10^{14} molecules cm^{-3} NO_2* was generated in the pulse. OH was not detected in these experiments. The results of an OH calibration experiment carried out immediately afterward enabled the sensitivity to be established under identical conditions. This was found to be 1×10^{-7} counts/s (cps) per [OH]. An upper limit to OH formation in the 532 nm excitation was obtained by fitting the scattered fluorescence signal to an exponential decay with a forced slope of 5300 s^{-1}, which corresponds to the expected decay rate of OH in the presence of 4.4×10^{15} cm^{-3} NO_2. The back-extrapolated signal at $t = 0$ was found to be 800 ± 600 cps. This is equivalent to about 8×10^9 OH cm^{-3}. Taking the relative efficiencies of quenching of NO_2 by Ar and H_2O and the relative concentrations of H_2O and Ar, it can be calculated that for this experiment 53% (1.4×10^{14} molecules cm^{-3}) of the NO_2* was quenched by H_2O. An upper limit of about $k_{10}/k_{12} = 8 \times 10^9/1.4 \times 10^{14} \approx 6 \times 10^{-5}$ can be placed on the relative contribution of OH formation in the quenching of NO_2* by water vapor. The value of 6×10^{-5} contains errors due to the estimation of NO_2* from joule meter reading of laser fluence at 532 nm, similar errors in the calculation of [OH] in the N_2O photolysis at 193 nm, and any errors associated with the relative rate constants for quenching of NO_2* by H_2O and Ar. Up until now we have used the data of ref 5 for the quenching rate constants (k_q(Ar) = 1.85×10^{-11} cm^3 molecule^{-1} s^{-1}). We note, however, that a value of 3.2×10^{-11} cm^3 molecule^{-1} s^{-1} for Ar quenching of NO_2* has been measured for 639 nm excitation.[27] Use of this quenching constant would result in 40% of NO_2* that is quenched by H_2O instead of 56%. The upper limit to the relative contribution of OH formation in the quenching of NO_2* by water vapor then becomes $\approx 7 \times 10^{-5}$.

Discussion

In the laser excitation experiments described above it was shown that the two-photon absorption of NO_2 at wavelengths between 430 and 450 nm is facile and leads to $O(^1D)$ production. We now examine the possibility that this can occur with sufficient efficiency in the troposphere to make it a significant source of $O(^1D)$. At a concentration of 1 ppb, the production rate of NO_2* is approximately $J_{EX}(NO_2)$*[NO_2] = 5×10^8 molecules cm^{-3} s^{-1}, and the loss rate, mainly due to collisional quenching (see above), is about 7×10^8 s^{-1}. The production and loss terms combine to result in a steady-state concentration of about 1.4 molecules cm^{-3}.

By assuming similar oscillator strengths for the NO_2* ← NO_2-($^2A_1$) and NO_2** ← NO_2* transitions as discussed above, and that the 2 $^2B_2$ state (NO_2**) dissociates to $O(^1D)$, we calculate a production rate of 2.8×10^{-2} molecules cm^{-3} s^{-1} for $O(^1D)$ by the process of sequential two-photon absorption by NO_2. A comparison with the $O(^1D)$ production rate via O_3 photolysis of approximately 1×10^6 $O(^1D)$ cm^{-3} s^{-1} renders this process uninteresting for the atmosphere. Indeed, any reactions of NO_2* with species other than H_2O, O_2, and N_2 are unlikely to be of importance under atmospheric conditions due to their low abundance.

By assuming that the reactivity of the excited state of NO_2 formed by 532 nm excitation is applicable to the entire nondissociative part of the NO_2 spectrum, the value derived above of $k_{10}/k_{12} \approx 7 \times 10^{-5}$ (or $k_{10} \approx 1.2 \times 10^{-14}$ cm^3 molecule^{-1} s^{-1}) can be used to assess the potential significance of reaction 10 as a source of OH in the troposphere. Using eq iii and the conditions outlined in the Introduction, we derive an upper limit to the rate of OH formation of about 3×10^3 OH cm^{-3} s^{-1}, less than 2% of the production rate via O_3 photolysis.

Conclusions

The potential role of the reaction between NO_2* and H_2O as a source of OH in the troposphere has been assessed by exciting NO_2 at discrete wavelengths between 430 and 450 nm and at 532 nm. The experiments at 430−450 nm revealed a facile sequential two-photon process that leads, via $O(^1D)$, to OH. This process will be inefficient in the troposphere due to the low photolysis intensities and rapid collisional quenching of NO_2*. At 532 nm no OH production was observed, enabling an upper limit of about 7×10^{-5} to be placed on the relative rate constant for reactive quenching of NO_2* to nonreactive quenching (collisional) by H_2O. If the reactivity of NO_2* following excitation at this wavelength is representative of the entire nondissociative part of the NO_2 absorption spectrum, we place an upper limit of about 2% to formation of OH via reaction 10 in the troposphere when solar zenith angles are high.

Acknowledgment. We thank Paul Crutzen for proposing that the reaction of NO_2* with H_2O may be a source of tropospheric OH, thereby stimulating this research.

References and Notes

(1) Crutzen, P. J. Atmospheric Interactions-Homogeneous Gas Reactions of C, N and S containing compounds (and references therein). In *The Major Biogeochemical Cycles and Their Interactions*; Bolin, B., Cook, R. B., Eds.; 1983; Chapter 3, SCOPE 21.

(2) Crutzen, P. J. *Annu. Rev. Earth Planet. Sci.* **1979**, *7*, 443.

(3) Crutzen, P. J.; Gidel, L. T. *J. Geophys. Res.* **1983**, *88*, 6641.

(4) Hough, A. *J. Geophys. Res.* **1991,** *96*, 7352.

(5) Okabe, H. *Photochemistry of Small Molecules*; John Wiley and Sons: New York, 1978.

(6) Roehl, C. M.; Orlando, J. J.; Tyndall, G. S.; Shetter, R. E.; Vazquez, G. J.; Cantrell, C. A.; Calvert, J. G. *J. Phys. Chem.* **1994**, *98*, 7837 and references therein.

(7) Paech, F.; Schmiedl, R.; Demtröder, *J. Chem. Phys.* **1975**, *63*, 4369.

(8) Haas, Y.; Houston, P. L.; Clark, J. H.; Moore, C. B.; Rosen, H.; Robrish, P. *J. Chem. Phys*, **1975**, *63*, 4195.

(9) Donnelly, V. M.; Kaufman, F. *J. Chem. Phys.* **1977**, *66*, 4100.

(10) Busch, G. E.; Wilson, K. R. *J. Chem. Phys*. **1972**, *56*, 3638.

(11) LUTHER program (adapted from: Luther, F. M.; Gelinas, R. J. *J. Geophys. Res.* **1976**, *81*, 1125. Isaksen, I. S. A.; Midtbo, K.; Sunde, J. Crutzen, P. J. Institut Report Series, No. 20, Institut for Geofysikk, University of Oslo, 1976).

(12) Norrish, R. G. W. *J. Chem Soc.* **1929**, 1158, 1611.

(13) Dickinson, R. G.; Baxter, W. P. *J. Am. Chem. Soc.* **1928**, *50*, 774

(14) Creel, C. L.; Ross, J. *J. Chem. Phys.* **1976**, *64*, 3560.

(15) Jones, I. T. N.; Bayes, J. D. *J. Chem. Phys.* **1973**, *59*, 4836.

(16) Nizkorodov, S. A.; Makarov, V. I.; Khmelinskii, I. V.; Kotschubei, S. A.; Amosov, K. A. *Chem. Phys. Lett*. **1994**, *222*, 135.

(17) Zellner, R.; Hartmann, D.; Rossner, I. *Ber. Bunsen-Ges. Phys. Chem.* **1992**, *96*, 385.

(18) Pitts, J. N.; Sanhueza, E.; Atkinson, R.; Carter, W. P. L.; Winer, A. M.; Harris, W. H.; Plun, C. N. *Int. J. Chem. Kinet.* **1984**, *16*, 919 and references therein.

(19) Besemer, A. C.; Nieboer, H. *Atmos. Environ.* **1985**, *19*, 507.

(20) Akimoto, H.; Takagi, H.; Sakamaki, F. *Int. J. Chem. Kinet*. **1987**, *19*, 539.

(21) Crowley, J. N.; Campuzano-Jost, P.; Moortgat, G. K. *J. Phys. Chem.* **1996**, *100*, 3601.

(22) DeMore, W. B.; Sander, S. P.; Golden, D. M.; Hampson, R. F.; Kurylo, M. J.; Howard, C. J.; Ravishankara, A. R.; Kolb, C. E.; Molina, M. J. Chemical Kinetics and Photochemical Data for Use in Stratospheric Modeling, JPL Publication 94-26, Pasadena, 1994.

(23) Clyne, M. A. A.; Down, S. *J. Chem. Soc., Faraday Trans. 2* **1974**, *70*, 253.

(24) Uselman, W. A.; Lee, E. K. C. *J. Chem. Phys.* **1976**, *65*, 1948.

(25) Gerstmayr, J. W.; Harteck, P.; Reeves, R. R. *J. Phys. Chem.* **1972**, *76*, 474.

(26) Hakala, D.; Harteck, P.; Reeves, R. R. *J. Phys. Chem.* **1974**, *78*, 1583.

(27) Hakala, D. F.; Reeves, R. R. *Chem. Phys. Lett.* **1976**, *28*, 510.